International Journal of Engineering

Journal Homepage: www.ije.ir

# Numerical Study of Pure Electroconvection and Combined Electro-thermo-convection in Horizontal Channels

R. Gannoun, W. Hassen*, M. I. Elkhazen and M. N. Borjini

Unit of Metrology and Energy Systems, Department of Energetic, University of Monastir, Monastir, Tunisia

*PAPER INFO*

*Paper history:*
Received 16 March 2017
Received in revised form 04 May 2017
Accepted 07 July 2017

*Keywords*:
Heat Transfer
Electro-hydro-dynamic
Electro-thermo-convection
Numerical Simulation

*ABSTRACT*

Electrohydrodynamic effect on natural convection in horizontal channels is investigated from a numerical point of view. The EHD effect is induced by narrow strip electrodes placed at the bottom wall of the channel. The channel is subjected in a first stage only to the electric forces, and in a second stage to the simultaneous action of a temperature gradient and an electric field. The interactions between electric field, flow field and temperature field are analyzed. It can be concluded that charge density distribution, flow pattern and temperature distribution are substantially affected by the arrangement of the electrodes; in fact four different arrangement were treated. The effect of pure electroconvection on charge density distribution and on flow pattern was studied. A periodic flow corresponding to particular values of electric Rayleigh was observed, then the impact of combined electro-thermo convection on heat transfer was undertaken in a second step and it was noted that the optimum arrangement of the electrodes provides an increase in heat transfer of up to 13%. The effect of the applied electric forces is also studied in order to highlight the importance of putting compromise between the supplied voltage and arrangement of the electrodes. Finally, a study of optimized configuration of electrodes was achieved.

***doi**: 10.5829/ije.2017.30.08b.21*

## 1. INTRODUCTION

It has been long known that applying an electric field to an insulated dielectric fluid which yields electrohydrodynamic forces in the fluid [1-3] is one of the most promising techniques among various active methods in heat transfer enhancement [4-7]. This method consists of the interactions between electric, flow and temperature fields. In fact, this technique is encountered in many industrial applications such as heat exchangers, solar heating systems, solar chimneys as well as cooling of electronic equipment. There exist some studies related to the use of EHD. For instance, using a computational fluid dynamics technique Kasayapanand and Kiatsiriroat [8] studied corona wind augmented heat transfer. Some authors [9-12] showed the EHD phenomenon in natural convection. Many theoretical and experimental studies have characterized the structure of the electroconvective flow in channels [13-18]. W. Hassen et al. [19] studied the effect of a partial unipolar injection on heat transfer in a horizontal annulus; their work aimed to eliminate the dead zone which is a poor exchange domain located at the bottom of the annular space. R.B Lakeh [20] has undertaken a computational and experimental approach to study heat transfer in parallel plate configuration using an electrically-induced secondary flow field. Also, F.S. Moghanlou et al. [21] carried out an experimental research on electrohydrodynamically induced heat transfer enhancement in a mini channel. S. Nasirivatan [22] focused on the effect of corona wind on the natural convection at absorber of a solar chimney; their experimental results showed the improvement of the efficiency of absorbers through enhanced heat transfer with corona wind. On the other side, the study of electrodes' arrangement effect on heat transfer was undertaken by N. Kasayapanand [23] as well as by M. Peng et al. [24] in a more recent research, but these studies focused only on the effect of punctual electrodes

*Corresponding Author's Email: *Hassen.walid@gmail.com* (W. Hassen)

Please cite this article as: R. Gannoun, W. Hassen, M. I. Elkhazen and M. N. Borjini, Numerical Study of Pure Electroconvection and Combined Electro-thermo-convection in Horizontal Channels, International Journal of Engineering (IJE), TRANSACTIONS B: Applications Vol. 30, No. 8, (August 2017) 1270-1278

placed inside the channels. In this study we will be interested on narrow strip electrodes placed at the bottom wall of a horizontal channel. In fact, the full numerical solutions of equations that model the EHD are very rare, especially in the horizontal channels; also the study of the combined effect of the electric Rayleigh and thermal Rayleigh for this type of geometry is almost nonexistent.

## 2. MATHEMATICAL FORMULATION AND NUMERICAL MODEL

We consider a dielectric fluid layer confined in a horizontal channel of length L, width W and aspect factor equal to 4, of which the two vertical walls are thermal insulators. The ground plate is maintained at constant temperature and the bottom wall is considered as heat transfer surface (subjected to hot temperature). The emitter narrow strip electrodes $(e = L/30)$ placed on the bottom wall (subjected to the variation of their arrangements) are held at potential V1 and represents the source of ions injection. The entire top wall is designed to absorb these injected ions and is held at potential $V_0$ (Figure 1). The layer is thus subjected simultaneously to a thermal gradient and a potential difference $\Delta V=V_1-V_0$. The problem is formulated considering the usual hypotheses of Newtonian and incompressible fluid of kinematic viscosity "ν", density "ρ", permittivity "ε" and thermal diffusivity "a".

The injection of charge of mobility "K" at the emitter is assumed 'homogeneous' and 'autonomous. In addition, to avoid excessive complexity, we neglect Joule heating. Finally, we consider the Boussinesq approximation. The general set of equations expressing the conservation of mass and momentum (the Navier-Stokes equations) including electrical and buoyancy forces, energy conservation, charge density conservation, the Gauss theorem and the definition of the electric field takes the form [25]:

$$\nabla.\vec{U}' = 0 \tag{1}$$

$$\rho_0\left(\frac{\partial\vec{U}'}{\partial t'} + (\vec{U}'.\nabla)\vec{U}'\right) = -\vec{\nabla}P' + +\rho\vec{g}\beta(\theta' - \theta_0) + \vec{f} + \mu\left(\frac{\partial^2 U_i'}{\partial^2 x_j'^2} + \frac{\partial^2 U_j'}{\partial^2 x_i'^2}\right) \tag{2}$$

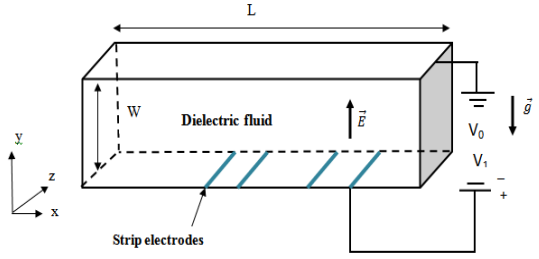


**Figure 1.** Problem geometry

$$\left(\frac{\partial\theta'}{\partial t'} + \vec{U}'.\nabla\theta'\right) = \nabla.(a\ \nabla\theta') \tag{3}$$

$$\frac{\partial q'}{\partial t'} + \nabla.\vec{j} = 0 \tag{4}$$

$$\nabla.(\varepsilon\vec{E}') = q' \tag{5}$$

$$\vec{E}' = -\vec{\nabla}V' \tag{6}$$

In Equation (2), $\vec{f}$ is the electric force

$$\vec{f} = q'E' - \frac{1}{2}E'^2\vec{\nabla}\varepsilon + \vec{\nabla}\left(\frac{1}{2}\rho E'^2\left(\frac{\partial\varepsilon}{\partial q'}\right)_\theta\right) \tag{7}$$

In Equation (4), $\vec{j}$ represents the current density which is defined as:

$$\vec{j} = q'\left(\vec{U}' + K\vec{E}'\right) \tag{8}$$

In Equation (7), the first term known as Coulomb force, is the force per unit volume exerted by electric field on a medium containing free charges. Under D.C. conditions, the second term corresponds to the dielectric force and it is very weak compared to the Coulomb force. The third term which represents the effect of electrostriction has the gradient form and can be included in the pressure term of momentum equation, but in the case of incompressible fluid this term can be also neglected [26-28]. Thus, finally the electric force can be expressed as:

$$\vec{f} = q'E' \tag{9}$$

As numerical method we had recourse to the "Vorticity-Stream function" formalism (ψ-ω), which allows the elimination of the pressure which is always tricky to handle. They are respectively defined by the two following relations:

$$\vec{\omega}' = \nabla\times\vec{u}' \tag{10}$$

$$\vec{u}' = \nabla\times\vec{\psi}' \tag{11}$$

Introducing the following dimensionless variables:

$$x = \frac{x'}{L} \quad y = \frac{y'}{L} \quad U_y = U_y'\frac{L}{a} \quad U_x = U_x'\frac{L}{a} \quad \psi = \frac{\psi'}{a}$$

$$\omega = \omega'\frac{L^2}{a} \quad t = t'\frac{a}{L^2} \quad \theta = \frac{\theta' - \theta_h}{\theta_c - \theta_h} \quad q = \frac{q'}{q_0}$$

$$E = E'\frac{L}{(V_1 - V_0)} \quad V = \frac{(V' - V_0)}{V_1 - V_0}$$

That leads to the definition of the following dimensionless numbers:

$$Ra = \frac{g\,\beta\,\Delta\theta\,L^3}{\nu\,a} \qquad Pr = \frac{\nu}{a} \qquad T = \frac{\varepsilon\,\Delta V}{\rho\,\nu\,K}$$

$$C = \frac{q\,L^2}{\varepsilon\,\Delta V} \qquad R = \frac{T}{M^2}$$

Which are respectively the thermal Rayleigh number, the Prandlt number, the ratio between the Coulomb and the viscous forces (called electric Rayleigh number), the measure of the injection strength, the mobility parameter which takes into account electro-hydrodynamic properties of the fluid and the electric Reynolds number.

For a two-dimensional geometry, the system which governs this type of electro-thermo-convective flow (1)-(6) is written in dimensionless form as:

$$\omega = -\left(\frac{\partial^2\Psi}{\partial x^2} + \frac{\partial^2\Psi}{\partial y^2}\right) \tag{12}$$

$$\frac{\partial\omega}{\partial t} + U_x\frac{\partial\omega}{\partial x} + U_y\frac{\partial\omega}{\partial y} = \frac{\partial^2\omega}{\partial x^2} + \frac{\partial^2\omega}{\partial y^2} + Ra.Pr.\frac{\partial\theta}{\partial x} + \frac{CT^2}{M^2}Pr^2\left(\frac{\partial(qE_y)}{\partial x} - \frac{\partial(qE_x)}{\partial y}\right) \tag{13}$$

$$\frac{\partial\theta}{\partial t} + U_x\frac{\partial\theta}{\partial x} + U_y\frac{\partial\theta}{\partial y} = \left(\frac{\partial^2\theta}{\partial x^2} + \frac{\partial^2\theta}{\partial y^2}\right) \tag{14}$$

$$\frac{\partial q}{\partial t} + \frac{\partial}{\partial x}\left(q\left(U_x + R.Pr.E_x\right)\right) + \frac{\partial}{\partial y}\left(q\left(U_y + R.Pr.E_y\right)\right) = 0 \tag{15}$$

$$\frac{\partial^2 V}{\partial x^2} + \frac{\partial^2 V}{\partial y^2} = -C\cdot q \tag{16}$$

$$E_y = -\frac{\partial V}{\partial y} \tag{17}$$

$$E_x = -\frac{\partial V}{\partial x} \tag{18}$$

To quantitatively evaluate the enhancement in heat transfer, the local and mean Nusselt numbers are defined at bottom wall as follow:

$$\overline{Nu} = \frac{1}{L}\int_0^L Nu\;\partial x \quad \text{where} \quad Nu = \left.\frac{\partial\theta}{\partial y}\right|_{y=0} \tag{19}$$

The boundary conditions are as follows:
At the bottom wall (At the electrodes)

$$\Psi = \frac{\partial\Psi}{\partial y} = 0\,,\quad V = q = \theta = 1,\quad \omega = -\frac{\partial^2\Psi}{\partial y^2} \tag{20}$$

At the bottom wall (Out electrodes)

$$\Psi = \frac{\partial\Psi}{\partial y} = \frac{\partial V}{\partial y} = \frac{\partial q}{\partial y} = 0\,,\ \theta = 1,\ \ \omega = -\frac{\partial^2\Psi}{\partial y^2} \tag{21}$$

At the top wall

$$\Psi = \frac{\partial\Psi}{\partial y} = V = \frac{\partial q}{\partial y} = 0\,,\ \theta = 1,\ \ \omega = -\frac{\partial^2\Psi}{\partial y^2} \tag{22}$$

At left and right walls

$$\Psi = \frac{\partial\Psi}{\partial x} = \frac{\partial V}{\partial x} = \frac{\partial q}{\partial x} = \frac{\partial\theta}{\partial x} = 0\ ,\ \ \omega = -\frac{\partial^2\Psi}{\partial x^2} \tag{23}$$

The partial differential Equations (12)-(16) governing the EHD flow field and the associate boundary condition (20)-(23) are integrated over a control volume. The power-law scheme for treating convective terms [29] is chosen for stability contingencies and in order to prevent excessive numerical diffusion, also a fully implicit first order Euler time scheme is retained to discretize the temporal derivatives [30], then a set of algebraic equations for the vorticity, stream function, energy, charge density and electric potential is obtained. This algebraic set of equations was solved using Successive Over Relaxation (SOR) based on the Gauss-Seidel iterative solver [31].

The choice of the relaxation coefficients for each unknown Ψ, ω, V, θ and q depends mainly on electric Rayleigh number. At high electric Rayleigh number, to avoid the divergence of the computation Ψ, ω, V, θ and q are under-relaxed. At low electric Rayleigh number in order to accelerate the calculation, Ψ is over-relaxed while ω, V, θ and q are under-relaxed.

Grid independency checks were performed and a 31 x 121 control volumes was found sufficient enough for the desired accuracy. Finer meshes have been tested without showing greater improvement of the results. The dimensionless time step was chosen equal to $10^{-4}$ which ensured the stability of the computations [32].
The stopping criterion is satisfied as soon as:

$$\frac{\max\left|\psi^K - \psi^{K-1}\right|}{\max\left|\psi^K\right|} + \max\left|q^K - q^{K-1}\right| \le 10^{-5} \quad \text{for each time step}$$

where the superscript k designates the $k^{th}$ iteration of the SOR algorithm. Finally, it is also noted that the dimensionless parameters used for these simulations are: Ra=10000, Pr=10, M=10 and C=10 corresponding to the strong injection case.

## 3. RESULTS AND DISCUSSION

### 3. 1. Pure Electroconvection

**3. 1. 1. Charge Density Distribution** Figure 2 investigates the charge density distribution for pure electroconvection case. When a potential difference is

applied, it is found that there is a formation of different mushroom structures around the electrodes' strips. In fact the formed mushroom structures are explained by the charge migration from the emitting wall to the receiving wall. Thus, the receiving wall is also gaining charges. On the other hand, it is seen that it is not covered with charges in the same way which is due to the different arrangement of the electrodes. It is observed that the highest concentration of charges remains always close to the electrodes. For the first configuration we observe two conjugated mushrooms that extend by increasing T. The charges always follow the location of the electrodes; that is why when the electrodes are spaced (2nd configuration), two clearly separated mushrooms are observed. It is noted also that the charges of the right mushroom have a greater longitudinal diffusion than those of the left one. In what regards the third arrangement of the electrodes, we observe also two conjugated mushrooms covering the central part of the channel, and the charges are more accumulated when T increases. For the fourth configuration, the longitudinal diffusion is limited and the charges are immediately dragged by high Coulomb force to the top wall. For this same configuration, we notice also that the charge plumes get slimmer when T is increased and the receiving wall is gaining more charges. In fact, the increase of the electric Rayleigh tilts in favor of convective forces rather than diffusive ones. It is also worth noting the symmetrical behavior for the two last configurations.

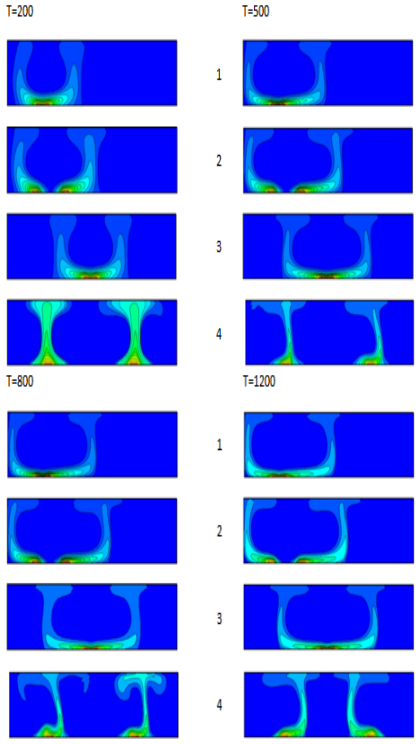


**Figure 2.** Charge density distribution for pure electro-convection

**3. 1. 2. Stream Function Contours** It is noted that the arrangement of the electrodes remarkably influences the flow structure while being dependent on the applied potential difference as well.

A multicellular flow with counter-rotating cells appears (Figure 3); for the first two configurations, three cells are obtained. However, for the first and second configurations, it is observed that the cells expand and the maximum vortex speed rotation increases. With respect to the third and fourth configuration, the cells number increases (4 cells) while covering the entire channel. It should be noted also that the flow rotation direction of these two last configurations has been inverted by comparing it with that of the first two configurations (upward at the extremities and downward in the center). On the other hand, the size of the cells and the maximum vortex rotational speed increased for the fourth configuration. For this same arrangement of the electrodes and for T=500 and T= 800, an unsteady flow is observed, the details of this flow are presented in the next paragraph.

**3. 1. 3. Periodic Flow** Indeed, a periodic regime is observed as it can be seen in Figure 4. The amplitude spectrum depicted in Figure 5 confirms the existence of a fundamental frequency equal to $f_1$=12.81, with mainly one higher harmonic ($f_2$=2 $f_1$).

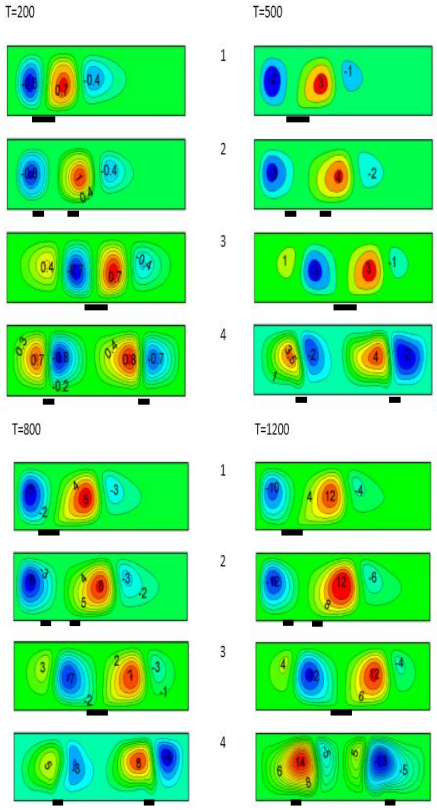


**Figure 3.** Stream function contours for pure electro-convection

To deeply study the behavior of the flow and the charge density, Figures 6 and 7 illustrate respectively a time sequence of streamlines and charge density distribution over one oscillation period (noted as τ). A phenomenon of cellular beat is observed in the figure; during this phenomenon, the cells are keeping almost the same shape and the same flow direction. Also, the maximum vortex speed rotation is seen at the beginning of the period, then it starts to decrease progressively to reach a minimum vortex speed rotation at the half of the period. From the half-period (at t+3τ/4), we observe that the cells are identical to the ones seen for t+τ/4, what allows to obtain almost the same structure as that of the beginning. On the other hand, in what regards the charge density distribution, an important longitudinal diffusion is observed near the electrodes. Then the plumes become narrower and the concentration of charges reaching the top wall is almost negligible. Then, the plumes become slimmer before being drifted to the top wall. Subsequently, the right plume widens, and the upper corresponding wall is almost void of charge. The left plume is, on the other hand, narrower and the concentration of charges at the receiving wall is much greater. At the half-period, longitudinal charge diffusion is great near the electrodes, the plumes had stopped diffusion at approximately y=0.5.

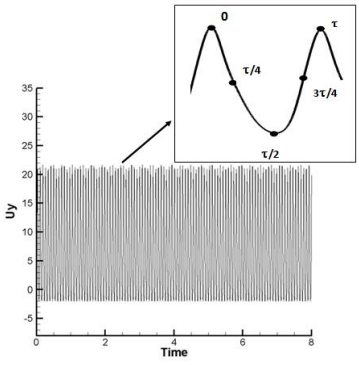


**Figure 4.** Time history of y velocity for pure electro-convection for C=10, M=10, T=800, x=0.25, y=0.3

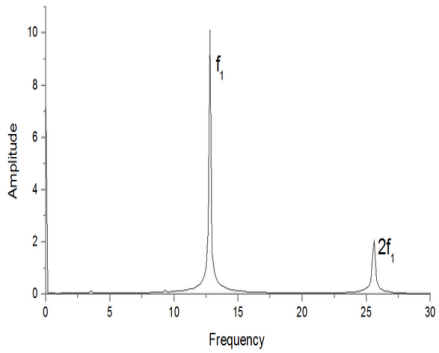


**Figure 5.** Amplitude spectrum of the longitudinal velocity for pure electroconvection for C=10, M=10, T=800

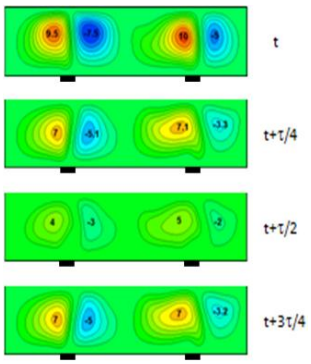


**Figure 6.** Streamline sequences during one main period (τ)

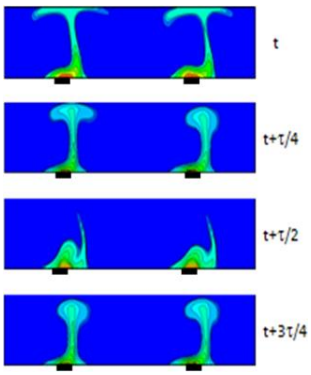


**Figure 7.** Charge density distribution during one main period (τ)

Towards the end of the period, the obtained plumes are almost identical to those observed at t+τ/4; however, they have not reached the receiving wall.

**3. 2. Combined Electrothermoconvection** The number of electrodes fixed to perform this work is 2 and four different arrangements were studied.

**3. 2. 1. Charge Density Distribution** Figure 8 investigates the charge density distribution of EHD applying while the Rayleigh number is fixed at $10^4$. It is noted that the highest concentration of charges remains always close to the electrodes. For the first arrangement (Figure 8.1), we notice only for a low potential difference that we obtain two conjugated mushrooms with charges covering the entire vertical left wall, but only a very small portion of the receiving wall is covered with charges. When T is increased, the same structure is found; there is lateral charge diffusion on the emitting wall increasing proportionally with T. The charges cover particularly the surface close to the electrodes and then are drifted to the top wall. Once the upper wall is reached, the increase of the electric Rayleigh value has no longer any effect on the lateral diffusion of charges on this wall. In what regards the second electrodes arrangement (Figure 8.2), we observe one mushroom structure which becomes wider when

increasing T to end by covering nearly the half of the channel for T= 1200. It is observed also that the structure of the mushroom follows the location of the electrodes; so, we can clearly see two mushrooms. In fact, for small values of T, the potential difference is not sufficiently high to control the distribution of charges and it is influenced essentially by the thermal forces. In the third configuration (Figure 8.3), we observe also two mushrooms covering the central portion of the channel with a size that expands by increasing T. For the fourth arrangement (Figure 8.4) and for T=200, two separated mushrooms covering the entire channel are obtained, a small portion of the emitting wall remains void of charges. While a very small portion of the receiving wall is covered with charges. Increasing T allows the narrowing of the surface covered with charges of the emitting wall (except for T=800, 3 mushrooms are obtained covering the entire emitting wall with charges) while receiving wall is still gaining more charges. Indeed for great values of T, there is little diffusion of charges which are immediately drifted to the receiving wall by thermo convective flow.

**3. 2. 2. Stream Function Contours** At first, it should be noted that the application of a thermal gradient causes a multicellular flow that covers the entire channel regardless of the configuration and also regardless of the electric Rayleigh number. For the pure thermo convective case, we obtain four perfectly symmetrical cells with a circular shape. By applying an electrical field, it is noted that the number of cells can reach a maximum of six, regardless of the value of T (except for T = 1200) (Figure 9). On the other hand it is noteworthy that the arrangement of the electrodes remarkably influences the flow structure, while being dependent on the applied potential difference as well; for instance, for the first arrangement, the maximum number of cells is obtained for T=200 (5 cells). For higher values of T we observe that the direction of the flow is reversed. An ascending flow in the vicinity of electrodes is thus obtained. The maximum vortex rotational speed increases and there is a coalescence of the two cells close to the electrodes when T increases. For the second arrangement, also the maximum number of cells is obtained for lower values of T (T=200 and T=500) three cells on the electrodes at the first half of the channel, but a new coalescence is seen in the second half of the channel for higher values of T and we obtain four cells having a shape which tends to be circular. For the last two configurations, symmetrical cells are always obtained with respect to the median of the channel. For the third configuration, six cells are observed for T=200. For the same T for the fourth arrangement, we note that there is an upward flow due to a thermal dominated zone. For higher values of T, we notice that the direction of flow in the vicinity of the electrodes has been inverted and the flow becomes descending. There are six cells for lower values of T. However, when T is increased, a coalescence of cells is obtained; so, we find 5 cells for T=800 and when T reaches 1200, a doubled coalescence is seen with 4 cells with a much with a much higher vortex rotation speed.

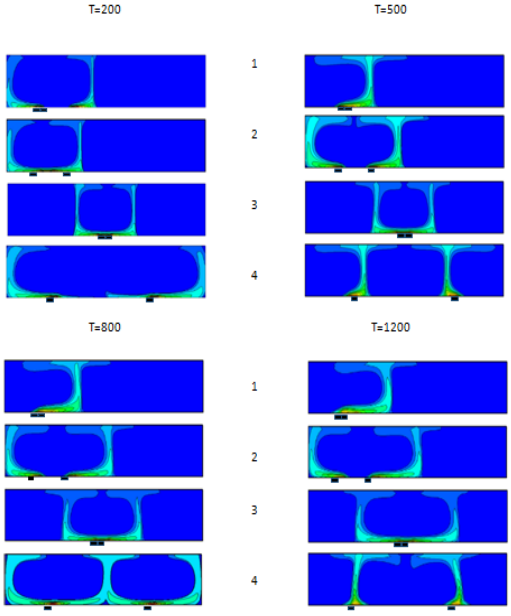


**Figure 8.** charge density distribution for combined electro-thermo-convection ($Ra=10^4$)

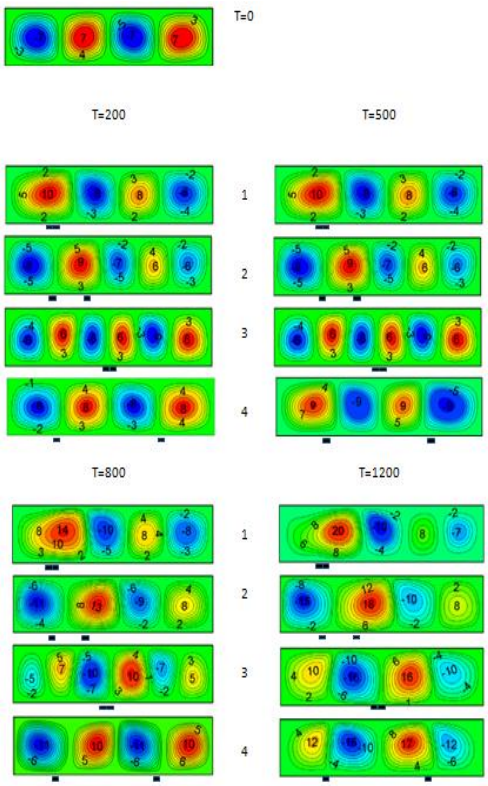


**Figure 9.** Stream function contours ($Ra= 10^4$)

The number of cells remains constant for the fourth configuration of electrodes. Indeed, when the potential difference becomes very important, obviously the electric force will have more influence and it will contribute with the simultaneous action of thermal forces to increase the maximum speed of the vortex rotation on the one hand, and will cause the coalescence of cells on the other hand, which become, thus, much wider.

**3. 2. 3. Temperature Distribution** The same temperature profile (Figure 10) is obtained for different electric Rayleigh numbers; however the larger thermal plumes remain approximate to the electrodes, while similar thermal plumes are found in the case of pure thermoconvection. Thus, the combined action of electric forces and buoyancy forces lead to the distortion of isotherm lines. On the other hand, the arrangement of the electrodes causes different temperature patterns to occur in the channel. Regardless of the value of T, we always obtain a maximum number of thermal plumes equal to 3 (for the second arrangement for T=200, for the third arrangement for T=500 and also for T=800. An unstable solution appears also for T=800 (downward hot fluid flow), for the third case. However, for this same configuration, for T=1200 a return to stability is seen and for any arrangement of the electrodes, we obtain much distorted isotherm lines with always two large thermal plumes.

**3. 2. 4. Heat Transfer** Figure 11 shows the evolution of the mean Nusselt number as a function of electric Rayleigh for the different arrangement of the electrodes treated in this study.

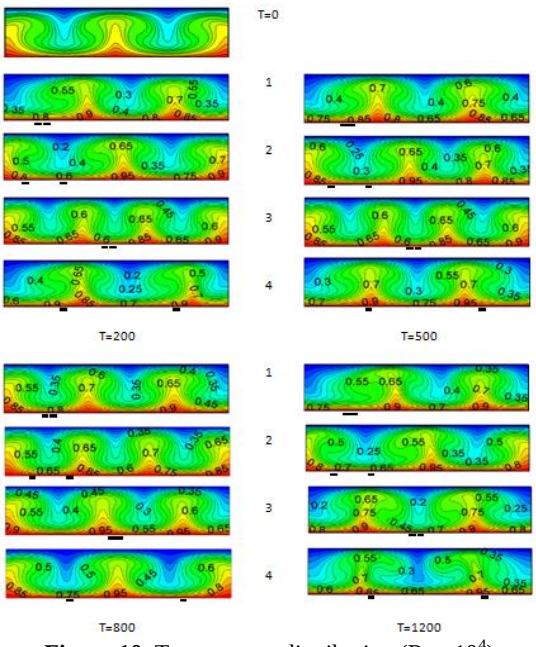


**Figure 10.** Temperature distribution (Ra= $10^4$)

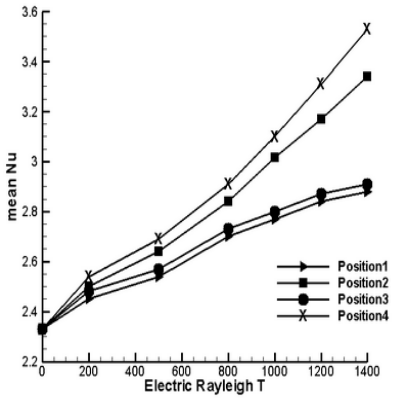


**Figure11.** Evolution of the mean Nusselt number as a function of electric Rayleigh for different arrangement of the electrodes.

It is observed that the application of an electric field greatly contributes to heat transfer enhancement; there is a 42% increase compared to the case of conventional natural convection and electrothermoconvective case with T = 1200. On the other hand, positioning of electrodes has a very significant effect on heat transfer. In fact, the lowest Nusselt values are observed when the electrodes are bonded either symmetrically or not. Then, for high values of T, the symmetrically spaced electrodes allow to obtain the best heat transfer. In fact, the positioning of electrodes achieves a heat transfer improvement exceeding 16% (for T=1200).

**3. 3. Effect of Optimization of Arrangement of Electrodes On Heat Transfer** In this part, we added electrodes in precise positions based on the nature of the flow (upward or downward flow) while starting with the observation of the pattern obtained with Rayleigh Benard convection. Figure 12 indicates the variation of the stream function with the position. The numbers added on the figure indicate the eventual positions where electrodes were added. Table 1 below shows the different treated cases; the number of electrodes fixed for this study is two. Thermal Rayleigh is $10^4$ and for the study of heat transfer electric Rayleigh number was set equal to 1200. We note that heat transfer enhancement depends on the configuration of the electrodes. As we saw in the previous section and Table 2, we obtain a greater improvement of heat transfer when the electrodes are spaced (heat transfer improvement of over 37%). The increase in heat transfer for each case in Table 2 is calculated with respect to the average Nusselt number obtained for pure electro-thermo-convection. However, even with stuck electrodes, we get a considerable heat transfer for case No. 3 with electrodes arranged in position 7; what is interesting to see is that this same position associated with another electrode placed at the tip of the channel enables a significant improvement in heat transfer (case

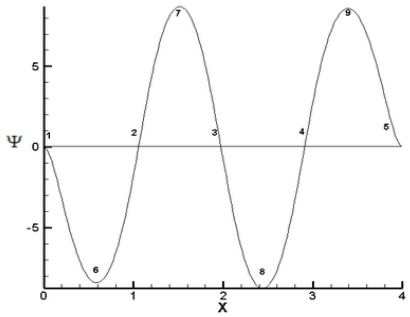


**Figure 12.** Variation of the stream function with the position (Rayleigh Benard convection, y=0.5)

**TABLE 1.** Treated cases with associated electrode's position

| Treated case | Electrode's position |
|---|---|
| **Joined electrode cases** | |
| 1 | 2 |
| 2 | 1 |
| 3 | 7 |
| 4 | 3 |
| **Spaced electrode cases** | |
| 5 | 7-8 |
| 6 | 6-8 |
| 7 | 2-7 |

**TABLE 2.** Effect of electrode's configuration on heat transfer

| Case | Average Nusselt | % of increase |
|---|---|---|
| 1 | 2.74 | 17.85 |
| 2 | 2.78 | 19.57 |
| 3 | 3.11 | 33.76 |
| 4 | 2.76 | 18.71 |
| 5 | 3.22 | 38.5 |
| 6 | 3.19 | 37.2 |
| 7 | 3.2 | 37.63 |

No. 6), however, the maximum heat transfer is achieved when the electrodes are placed at x = 1.52 (position 7) and x = 2.44 (position 8) which means for almost symmetrical electrodes with respect to the median of the channel and also in the intermediate position thus, generally we can conclude that injecting electrodes in vertically motionless areas allow to obtain the best heat transfer.

## 4. CONCLUSION

Numerical simulations are carried out to analyze the mechanism of natural convection inside horizontal channels incorporating with an electrohydrodynamic effect. The conclusions are as follow: A periodic flow was depicted in the case of pure electroconvection for T=500 and T=800. The flow pattern and charge density distribution are affected by the provided electric Rayleigh. The cooperation of thermal gradient and of an electric field allows the development of the flow along the whole channel which is not the case for pure electroconvection. Arrangement of the electrodes have considerable impact on the heat transfer; in fact bonded electrodes should be avoided since symmetrical spacing of the electrodes allows having an important enhancement in heat transfer. Optimizationof the arrangement of Electrodes confirms the results obtained above, but it also shows that there are some other configurations that should be avoided such as placing joined electrodes at the end of the channel (x=0.1 and x=1.08).

## 5. REFERENCES

1. Seyed-Yagoobi, J., "Electrohydrodynamic pumping of dielectric liquids", ***Journal of Electrostatics***, Vol. 63, No. 6, (2005), 861-869.
2. Atten, P. and Seyed-Yagoobi, J., "Electrohydrodynamically induced dielectric liquid flow through pure conduction in point/plane geometry", ***IEEE Transactions on Dielectrics and Electrical Insulation***, Vol. 10, No. 1, (2003), 27-36.
3. Hanaoka, R., Takata, S., Murakumo, M. and Anzai, H., "Properties of liquid jet induced by electrohydrodynamic pumping in dielectric liquids", ***Electrical Engineering in Japan***, Vol. 138, No. 4, (2002), 1-9.
4. Yabe, A., Mori, Y. and Hijikata, K., "Ehd study of the corona wind between wire and plate electrodes", ***AIAA Journal***, Vol. 16, No. 4, (1978), 340-345.
5. Velkoff, H. and Godfrey, R., "Low-velocity heat transfer to a flat plate in the presence of a corona discharge in air", ***Journal of Heat Transfer***, Vol. 101, (1979), 157-163.
6. Yamamoto, T. and Velkoff, H., "Electrohydrodynamics in an electrostatic precipitator", ***Journal of Fluid Mechanics***, Vol. 108, (1981), 1-18.
7. Tada, Y., Takimoto, A. and Hayashi, Y., "Heat transfer enhancement in a convective field by applying ionic wind", ***Journal of Enhanced Heat Transfer***, Vol. 4, No. 2, (1997).
8. Kasayapanand, N. and Kiatsiriroat, T., "Numerical modeling of the electrohydrodynamic effect to natural convection in vertical channels", ***International Communications in Heat and Mass Transfer***, Vol. 34, No. 2, (2007), 162-175.
9. Yan, Y., Zhang, H. and Hull, J., "Numerical modeling of electrohydrodynamic (ehd) effect on natural convection in an enclosure", ***Numerical Heat Transfer, Part A: Applications***, Vol. 46, No. 5, (2004), 453-471.
10. Sheikhzadeh, G., Arefmanesh, A., Kheirkhah, M. and Abdollahi, R., "Numerical study of natural convection in an inclined cavity with partially active side walls filled with cu-water nanofluid", ***International Journal of Engineering-Transactions B: Applications***, Vol. 24, No. 3, (2011), 279-288.
11. Saha, G., Saha, S., Hasan, M. and Islam, M.Q., "Natural convection heat transfer within octagonal enclosure", ***IJE Transactions A: Basics***, Vol. 23, No. 1, (2010), 1-10.
12. Maatki, C., Ghachem, K., Kolsi, L., Borjini, M. and Ben Aissia, H., "Entropy generation of double diffusive natural convection in a three dimensional differentially heated enclosure", ***International Journal of Engineering***, Vol. 2, (2014), 215-226.

13. Aung, W., "Fully developed laminar free convection between vertical plates heated asymmetrically", ***International Journal of Heat and Mass Transfer***, Vol. 15, No. 8, (1972), 1577-1580.
14. Bahrami, P. and Sparrow, E., "Experiments on natural convection from vertical parallel plates with either open or closed edges", ***Journal of Heat Transfer***, Vol. 102, (1980), 221-227.
15. Morrone, B., Campo, A. and Manca, O., "Optimum plate separation in vertical parallelplate channels for natural convective flows: Incorporation of large spaces at the channel extremes", ***International Journal of Heat and Mass Transfer***, Vol. 40, No. 5, (1997), 993-1000.
16. Lee, K.-T., "Natural convection heat and mass transfer in partially heated vertical parallel plates", ***International Journal of Heat and Mass Transfer***, Vol. 42, No. 23, (1999), 4417-4425.
17. Kasayapanand, N., "Enhanced heat transfer in inclined solar chimneys by electrohydrodynamic technique", ***Renewable Energy***, Vol. 33, No. 3, (2008), 444-453.
18. Hassen, W., Traore, P., Borjinia, M. and Aissiaa, H.B., "Numerical study of electro-thermo-convection in a differentially heated cavity filled with a dielectric liquid subjected to partial unipolar injection", ***International Journal of Engineering-Transactions C: Aspects***, Vol. 28, No. 9, (2015), 1343.
19. Hassen, W., Elkhazen, M.I., Traore, P. and Borjini, M.N., "Numerical study of the electro–thermo-convection in an annular dielectric layer subjected to a partial unipolar injection", ***International Journal of Heat and Fluid Flow***, Vol. 50, (2014), 201-208.
20. Lakeh, R.B. and Molki, M., "Enhancement of convective heat transfer by electrically-induced swirling effect in laminar and fully-developed internal flows", ***Journal of Electrostatics***, Vol. 71, No. 6, (2013), 1086-1099.
21. Moghanlou, F.S., Khorrami, A.S., Esmaeilzadeh, E. and Aminfar, H., "Experimental study on electrohydrodynamically induced heat transfer enhancement in a minichannel", ***Experimental Thermal and Fluid Science***, Vol. 59, (2014), 24-31.
22. Nasirivatan, S., Kasaeian, A., Ghalamchi, M. and Ghalamchi, M., "Performance optimization of solar chimney power plant using electric/corona wind", ***Journal of Electrostatics***, Vol. 78, No., (2015), 22-30.
23. Kasayapanand, N., "Electrode arrangement effect on natural convection", ***Energy conversion and management***, Vol. 48, No. 4, (2007), 1323-1330.
24. Peng, M., Wang, T.-H. and Wang, X.-D., "Effect of longitudinal electrode arrangement on ehd-induced heat transfer enhancement in a rectangular channel", ***International Journal of Heat and Mass Transfer***, Vol. 93, (2016), 1072-1081.
25. Hassen, W., Borjini, M., Traore, P. and Aissia, H.B., "Electroconvection between coaxial cylinders of arbitrary ratio subjected to strong unipolar injection", ***Journal of Electrostatics***, Vol. 71, No. 5, (2013), 882-891.
26. Atten, P. and Moreau, R., "Stabilite electrohydrodynamique des liquides isolants soumis a une injection unipolaire", ***Journal of Mecanique***, Vol. 11, No. 3, (1972), 471-521.
27. Atten, P. and Lacroix, J., "Non-linear hydrodynamic stability of liquids subjected to unipolar injection", ***Journal de Mécanique***, Vol. 18, (1979), 469-510.
28. El Moctar, A.O., Peerhossaini, H., Le Peurian, P. and Bardon, J., "Ohmic heating of complex fluids", ***International Journal of Heat and Mass Transfer***, Vol. 36, No. 12, (1993), 3143-3152.
29. Patankar, S., "Numerical heat transfer and fluid flow, CRC press, (1980).
30. Borjini, M.N., Abidi, A. and Aissia, H.B., "Prediction of unsteady natural convection within a horizontal narrow annular space using the control-volume method", ***Numerical Heat Transfer, Part A: Applications***, Vol. 48, No. 8, (2005), 811-829.
31. Bejan, A., "Convection heat transfer, John wiley & sons, (2013).
32. Vazquez, P., Georghiou, G. and Castellanos, A., "Numerical analysis of the stability of the electrohydrodynamic (ehd) electroconvection between two plates", ***Journal of Physics D: Applied Physics***, Vol. 41, No. 17, (2008), 175303.


# Numerical Study of Pure Electroconvection and Combined Electro-thermo-convection in Horizontal Channels


R. Gannoun, W. Hassen, M. I. Elkhazen and M. N. Borjini

Unit of Metrology and Energy Systems, Department of Energetic, University of Monastir, Monastir, Tunisia


*P A P E R I N F O*


*Paper history:*
Received 16 March 2017
Received in revised form 04 May 2017
Accepted 07 July 2017

*Keywords*:
Heat Transfer
Electro-hydro-dynamic
Electro-thermo-convection
Numerical Simulation


**چکیده**


اثر الکتروهیدرودینامیکی (EHD) بر روی گرایش طبیعی در کانال‌های افقی از دیدگاه عددی بررسی شده است. اثر EHD توسط الکترودهای نوار باریک قرار داده شده در دیوار پایین کانال ایجاد می‌شود. کانال در مرحله اول تنها به نیروهای الکتریکی و در مرحله دوم به اثر همزمان یک گرادیان درجه حرارت و یک میدان الکتریکی اعمال می‌شود. تعاملات بین میدان الکتریکی، میدان جریان و میدان دما تجزیه و تحلیل می‌شود. می‌توان چنین نتیجه گرفت که توزیع چگالی شار، الگوی جریان و توزیع دما به طور قابل ملاحظه-ای از آرایش الکترودها تأثیر می‌پذیرند. در واقع، چهار روش مختلف الکترود تحت مطالعه قرار گرفتند. اثر الکتروشیمیایی خالص بر توزیع تراکم شارژ و الگوی جریان مطالعه شده است. یک جریان دوره‌ای که مربوط به مقادیر ویژه الکتریکی رایلی بود، مشاهده شد. اثر ترکیب الکتریکی حرارتی در انتقال حرارت در مرحله دوم بررسی و مشاهده شد که ترتیب الکترودهای بهینه افزایش انتقال حرارت تا ۱۳٪ را فراهم می‌کند. اثر نیروهای الکتریکی اعمال شده نیز مورد توجه قرار گرفته است تا اهمیت مصالحه بین ولتاژ تامین شده و تنظیم الکترود را برجسته نماید. در نهایت، مطالعه پیکربندی الکترود بهینه شده به دست آمد.



***doi**: 10.5829/ije.2017.30.08b.21*